Interplay between electron-phonon and electron-electron interactions

O. Rösch[1], **J. E. Han**[2], **O. Gunnarsson**[*1], and **V. H. Crespi**[3]

[1] Max-Planck-Institut für Festkörperforschung, D-70506 Stuttgart, Germany
[2] Department of Physics, State University of New York, Buffalo, NY 14260, USA
[3] Department of Physics, The Pennsylvania State University, University Park, PA 16802-6300, USA

Received zzz, revised zzz, accepted zzz
Published online zzz

PACS 74.70.Wz,74.72.-h,63.20.Kr,71.10.Fd,63.22.+m,71.70.Ej

We discuss the interplay between electron-electron and electron-phonon interactions for alkali-doped fullerides and high temperature superconductors. Due to the similarity of the electron and phonon energy scales, retardation effects are small for fullerides. This raises questions about the origin of superconductivity, since retardation effects are believed to be crucial for reducing effects of the Coulomb repulsion in conventional superconductors. We demonstrate that by treating the electron-electron and electron-phonon interactions on an equal footing, superconductivity can be understood in terms of a local pairing. The Jahn-Teller character of the important phonons in fullerides plays a crucial role for this result. To describe effects of phonons in cuprates, we derive a t-J model with phonons from the three-band model. Using exact diagonalization for small clusters, we find that the anomalous softening of the half-breathing phonon as well as its doping dependence can be explained. By comparing the solution of the t-J model with the Hartree-Fock approximation for the three-band model, we address results obtained in the local-density approximation for cuprates. We find that genuine many-body results, due to the interplay between the electron-electron and electron-phonon interactions, play an important role for the the results in the t-J model.

1 Introduction

The effects of electron-phonon interactions are often studied in models with no electron-electron interaction, due to the difficulty of treating both interactions simultaneously [1]. For some systems of interest this is a quite questionable approximation. Here we address (i) alkali-doped fullerides and (ii) high-T_c cuprates, where the Coulomb interaction is important. We illustrate that there is an interesting and important interplay between these two types of interactions for such systems.

The alkali-doped fullerides are characterized by a very unusual parameter range, where the energy scales for phonons and electrons are comparable [2]. This has important consequences for the understanding of superconductivity. For conventional superconductors, it is argued that the Coulomb repulsion has a small effect on superconductivity due to retardation effects. These effects are usually described by a small empirical Coulomb pseudopotential μ^*. Due to the smallness of this parameter, the rather weak, phonon-induced attraction between the electrons can drive superconductivity. For alkali-doped fullerides there is no reason to assume strong retardation effects, due to the similarity of the electron and phonon energy scales. There is then also no reason to assume that μ^* is small for these system or to treat it as an empirical parameter. Instead, the electron-phonon and electron-electron interactions ought to be treated on the same footing. Conventional superconductors are usually treated in the Migdal-Eliashberg theory, assuming that the phonon energies are very small on the electronic energy scale. For alkali-doped fullerides, Migdal's

* Corresponding author: e-mail: O.Gunnarsson@fkf.mpg.de, Phone: +49 711 689 1669, Fax: +49 711 689 1632

theorem is very questionable, and we would like to avoid the use of this theorem. Both these objectives can be achieved [3] by using the dynamical mean-field theory [4]. We find that superconductivity in alkali-doped fullerides is due to an interplay between the electron-phonon and electron-electron interaction. In particular, it is crucial that the important coupling is due to Jahn-Teller H_g phonons. We find that for coupling to symmetric A_g phonons, the transition temperature T_c drops quickly as the Coulomb repulsion U is increased, while this is not the case for coupling to H_g phonons. The theory [3] can describe the strong doping dependence observed experimentally.

For high-T_c cuprates there has been much interest in the electron-phonon interaction after Lanzara *et al.* [5] found a strong interaction to a mode at 70 meV in their photoemission spectroscopy (PES) work. This was interpreted as a strong coupling to a half-breathing phonon, where the bond between a Cu atom and two surrounding O atoms is stretched. This phonon is anomalous, in the sense that it is rather strongly softened and acquires a large width under doping [6, 7, 8, 9] in a way which cannot easily be described in a shell model. On the other hand, although the energy of this phonon is well described in local density approximation (LDA) band structure calculations [10], its coupling is found to be very weak, $\lambda \sim 0.01$ [11, 10]. This suggests that it might be important to take into account the strong electron-electron interactions also in this case. This can be done by using the t-J model [12] and by including the interaction with phonons [13, 14, 15, 16].

The t-J model is derived from the three-band model [17] by projecting out states with two Cu $3d$-holes or with extra O $2p$-holes. In the doped system, the additional holes are assumed to mainly occupy O $2p$-states. These O $2p$-holes form Zhang-Rice singlets with the Cu $3d$-holes [12]. The singlet formation energy is very large, of the order of 4-5 eV. For a given doping and a rigid lattice, this large energy plays a small role, since it only enters as an uninteresting constant. The singlet energy is strongly modulated by the (half-)breathing phonons, however, since these strongly modulate the Cu-O hopping. We therefore find that the phonons couple strongly to the on-site energies of the t-J model via the coupling to the hopping integrals [16]. By using exact diagonalization for small clusters, we can determine [16] the phonon softening and find that it is of the right order of magnitude, has the correct doping dependence, and is weaker for the breathing phonon than the half-breathing phonon, as it should be.

To make contact to the LDA band structure calculations, we study the three-band model in the Hartree-Fock (HF) mean-field approximation. This approximation is expected to behave in a similar way as the LDA for the doped, paramagnetic state, but it has the advantage that it allows an antiferromagnetic insulating solution for the undoped system. In this case we can determine the softening under doping in the HF approximation of the three-band model. We find [18] that although the softening is comparable to what is found in the t-J model, the underlying physics is different. We also find that the doping and $\boldsymbol{q}$-dependence in the HF approximation of the three-band model is different from the t-J model, and in worse agreement with experiment.

2 Alkali-doped fullerides

2.1 Model

To describe alkali-doped fullerides we introduce a model which contains the essential interactions

$$\begin{aligned} H &= \sum_{ijmm'\sigma} t_{ijmm'} \psi^{\dagger}_{im\sigma}\, \psi_{jm'\sigma} + U \sum_{i(\sigma m)<(\sigma' m')} n_{im\sigma}\, n_{im'\sigma'} \\ &\quad + \omega_{ph} \sum_{i\nu} b^{\dagger}_{i\nu} b_{i\nu} + g \sum_{imm'\sigma\nu} V^{(\nu)}_{mm'} \psi^{\dagger}_{im\sigma} \psi_{im'\sigma} (b_{i\nu} + b^{\dagger}_{i\nu}). \end{aligned} \tag{1}$$

Here the first term describes hopping integrals $t_{ijmm'}$ between the partly occupied three-fold degenerate t_{1u} levels, which are the important levels for doped C_{60}. All other levels are sufficiently far from the Fermi level to be assumed to be rather unimportant. The band width is W, i is a site index and m is an orbital index. The second term describes the Coulomb interaction U between two electrons on the same

C_{60} molecule. We only include a Hubbard U and neglect the terms giving a multiplet type of Hund's rule coupling. The important electron-phonon coupling is due to the coupling to eight five-fold degenerate intramolecular H_g phonons on each C_{60} molecule. Here we just consider one five-fold degenerate phonon per C_{60} molecule, which has the frequency ω_{ph} and the degeneracy index ν. The last term describes the electron-phonon coupling, where g gives the coupling strength and $V^{(\nu)}_{mm'}$ is determined by symmetry. We refer to this as the $t \times H$ model. As a comparison we also study an $a \times A$ model, where a nondegenerate level (with a symmetry) couples to a nondegenerate phonon (with A symmetry), and an $e \times E$ problem, where a two-fold degenerate level couples to a two-fold degenerate phonon.

2.2 Methods

To study superconductivity, we apply a weak perturbation which creates an electron pair

$$\Delta = \sum_{im} \psi^\dagger_{im\downarrow} \psi^\dagger_{im\uparrow}. \tag{2}$$

The response to this perturbation is described by the pairing susceptibility

$$\chi(\tau_1, \tau_2, \tau_3, \tau_4) = \frac{1}{N} \sum_{ijmm'} \langle T_\tau \psi_{im\uparrow}(\tau_1) \psi_{im\downarrow}(\tau_2) \psi^\dagger_{jm'\downarrow}(\tau_3) \psi^\dagger_{jm'\uparrow}(\tau_4) \rangle,$$

where $\langle ... \rangle$ denotes a thermal average, T_τ is a time-ordering operator, τ is an imaginary time, $\psi_{im\uparrow}(\tau)$ is an operator in the Heisenberg representation and N is the number of sites. Superconductivity is obtained if χ diverges at a temperature T_c, since the system can then sustain electron pairs without any external perturbation [19]. We Fourier transform χ with respect to $\tau_1 - \tau_2$ and $\tau_3 - \tau_4$ and introduce a Bethe-Salpeter equation

$$\chi = (\chi_0^{-1} - \Gamma)^{-1} = (1 - \chi_0 \Gamma)^{-1} \chi_0, \tag{3}$$

where

$$\chi_0(\tau_1, \tau_2, \tau_3, \tau_4) = \frac{1}{N} \sum_{mm'} \sum_{\boldsymbol{k}} G_{mm'}(\boldsymbol{k}, \tau_1 - \tau_4) G_{mm'}(-\boldsymbol{k}, \tau_2 - \tau_3) \tag{4}$$

describes two independently propagating fully dressed electrons (or holes) at zero net momentum and Γ is an effective interaction.

To perform calculations we use the dynamical mean-field theory (DMFT) [4]. The problem is replaced by an effective impurity problem, embedded in a self-consistently determined host. This leads to a $\boldsymbol{k}$-independent self-energy $\Sigma(\boldsymbol{k}, \omega)$. The impurity model is solved by using a Monte-Carlo approach [20]. The Coulomb interaction is treated by the discrete Hubbard-Stratonovich decoupling scheme, introducing auxiliary fields. The phonons are described by the displacement field

$$Q_{i\nu} \equiv (b^\dagger_{i\nu} + b_{i\nu})/\sqrt{2}, \tag{5}$$

which provides a fully quantum mechanical description. Both fields are sampled using a Monte-Carlo approach. This provides a treatment of the Coulomb and electron-phonon interactions on an equal footing and without any assumptions about Migdal's theorem.

Within DMFT, an approximation for the effective interaction Γ can be obtained by introducing a local pairing susceptibility

$$\chi^{\rm loc}(\tau_1, \tau_2, \tau_3, \tau_4) = \sum_{mm'} \langle T_\tau \psi_{m\uparrow}(\tau_1) \psi_{m\downarrow}(\tau_2) \psi^\dagger_{m'\downarrow}(\tau_3) \psi^\dagger_{m'\uparrow}(\tau_4) \rangle, \tag{6}$$

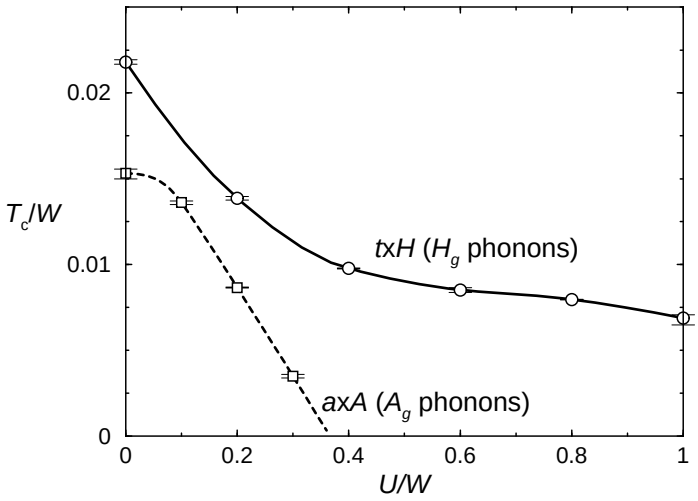

Fig. 1 T_c as a function of U. Results are shown for the $t \times H$ and $a \times A$ models for half-filling, using the parameters $\lambda = 0.6$ and $\omega_{ph}/W = 0.25$. The figure illustrates the important difference between H_g and A_g phonons (after Han *et al.* [3]).

where the response is measured on the same site as the site where the perturbation is applied. We introduce the Bethe-Salpeter equation for local quantities

$$\chi^{\mathrm{loc}} = [(\chi_0^{\mathrm{loc}})^{-1} - \Gamma^{\mathrm{loc}}]^{-1}, \tag{7}$$

where

$$\chi_0^{\mathrm{loc}}(\tau_1, \tau_2, \tau_3, \tau_4) = \sum_{mm'} G_{mm'}^{\mathrm{loc}}(\tau_1 - \tau_4) G_{mm'}^{\mathrm{loc}}(\tau_2 - \tau_3) \tag{8}$$

where $G_{mm'}^{\mathrm{loc}}(\tau_1 - \tau_2) = \sum_{\boldsymbol{k}} G_{mm'}(\boldsymbol{k}, \tau_1 - \tau_2)/N$ is a local electron Green function. Both χ^{loc} and χ_0^{loc} can be calculated within DMFT, and we can therefore obtain Γ^{loc}. We introduce the assumption that $\Gamma \approx \Gamma^{\mathrm{loc}}$. This is expected to be a good approximation, since the interaction is due to intramolecular phonons and an intramolecular Coulomb repulsion. Since χ_0 can be calculated within DMFT, χ follows from Eq. (3).

2.3 Results

Fig. 1 shows the transition temperature T_c as a function of the Coulomb repulsion U for the $t \times H$ and $a \times A$ models at half-fi lling. We fi rst consider the $a \times A$ result. In this case the effective electron-electron interaction is

$$\frac{U_{\mathrm{tot}}}{W} \approx -\frac{\pi}{4}\lambda + \frac{U}{W} = -0.47 + \frac{U}{W}, \tag{9}$$

where the fi rst term is the phonon induced attraction, which for $\lambda = 0.6$ is about $-0.47W$. For $U = 0$ this attraction leads to superconductivity with an appreciable T_c. As U is increased, the attractive interaction is reduced, and we would expect superconductivity to be lost when $U/W \sim 0.47$. Figure 1 shows that this does indeed happen, and superconductivity is actually suppressed even for somewhat smaller values of U. For the $t \times H$ case, the effective interaction is given by

$$\frac{U_{\mathrm{tot}}}{W} \approx -0.2 + \frac{U}{W}. \tag{10}$$

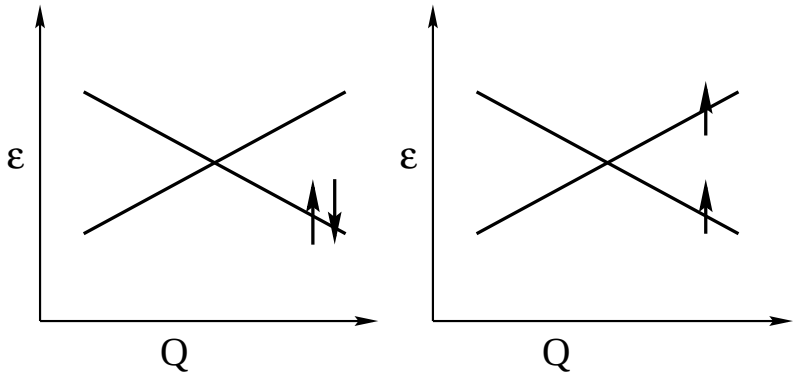

Fig. 2 Schematic illustration of the shifts of the e levels as a function of the phonon coordinate Q for an E phonon. The figure illustrates that the electron-phonon coupling favors a singlet (left hand side) over a triplet (right hand side).

The phonon induced attraction is weaker than for the $a \times A$ case due to strong-coupling effects [22], and one might have expected superconductivity to have been lost already at $U/W \sim 0.2$. Fig. 1 illustrates that T_c drops much more slowly, and that the superconductivity is surprisingly insensitive to the Coulomb repulsion. This is crucial for superconductivity in fullerides. In the following we discuss this dramatic difference between the $a \times A$ and $t \times H$ models.

2.4 Local pairing

We first consider $\Gamma^{\rm loc}$. Putting $\tau_1 = \tau_2$, $\tau_3 = \tau_4$ and taking the Fourier transform with respect to $\tau_1 - \tau_3$ in the $T \to 0$ limit, we obtain

$$\tilde{\chi}^{\rm loc}(i\omega_n) = \frac{1}{2\pi}\int_{-\infty}^{\infty} \frac{\rho^{\rm loc}(\varepsilon)}{i\omega_n - \varepsilon}, \tag{11}$$

where

$$\begin{aligned} \rho^{\rm loc}(\varepsilon) &= 2\pi \sum_n |\langle n, N-2| \sum_m \psi_{m\uparrow}\psi_{m\downarrow}|0,N\rangle|^2 \\ &\quad \times \delta[\varepsilon - E_0(N) + E_n(N-2)] + ... \end{aligned} \tag{12}$$

$|n,N\rangle$ is the nth excited state of the system with N electrons and the energy $E_n(N)$. The term shown describes the removal of an electron pair and "..." indicates the addition of an electron pair. The chemical potential μ has been put to zero. Here $\rho^{\rm loc}(\varepsilon) \leq 0$ for $\varepsilon > 0$ and $\rho^{\rm loc}(\varepsilon) \geq 0$ for $\varepsilon < 0$.

We consider the simplest case, the $e \times E$ problem at half-filling, where a two-fold degenerate level couples to a two-fold degenerate Jahn-Teller phonon. The excitation of an E phonon leads to a splitting of the previously two-fold degenerate level, as shown schematically in Fig. 2. The system then tends to put two electrons with opposite spins in orbitals with the same m-quantum numbers, a local pairing. This effect competes with the hopping between the molecules, which tends to put the electrons randomly into the molecular levels. However, if U is large, hopping is reduced. The Jahn-Teller effect can then dominate over hopping, and the system tends to go into a state where each molecule is in a singlet state (local pairing)

$$\frac{1}{\sqrt{2}} \sum_{m=1}^{2} \psi^{\dagger}_{m\uparrow}\psi^{\dagger}_{m\downarrow}|{\rm vac}\rangle. \tag{13}$$

Here the two electrons on a molecule tend to be in levels with the same m-quantum number but opposite spins. It is clear that an electron pair can then easily be annihilated from such a state, and we expect the

spectral function $\rho^{\rm loc}(\varepsilon)$ to have a large weight. Actually, there is a sum-rule in the limit of a large U and a strong electron-phonon coupling λ [3]

$$\frac{1}{2\pi}\int_{-\infty}^{\infty}|\rho^{\rm loc}(\varepsilon)|d\varepsilon \equiv P = 2. \tag{14}$$

This can be compared with the sum-rule for $\rho_0^{\rm loc}(\varepsilon)$ corresponding to $\chi_0^{\rm loc}$

$$\frac{1}{2\pi}\int_{-\infty}^{\infty}|\rho_0^{\rm loc}(\varepsilon)|d\varepsilon \equiv P_0 = 1. \tag{15}$$

Since this sum-rule corresponds to the case when the two electrons in $\chi_0^{\rm loc}$ do not interact with each other, they may be in states with different m-quantum numbers with a substantial probability. It is then harder to remove an electron pair, and the sum rule is correspondingly smaller. This tends to make $\chi^{\rm loc}$ larger than $\chi_0^{\rm loc}$. From Eq. (7) it follows that this tends to lead to an attractive $\Gamma^{\rm loc}$.

Since A_g phonons couple in the same way to all m-quantum numbers, they do not favor local pairing. This explains the important difference between the $t \times H$ and $a \times A$ models in Fig. 1. It is interesting that the Coulomb interaction actually helps local pairing. As mentioned above, hopping and local pairing compete. The Coulomb repulsion reduces hopping and helps local pairing to win over hopping. Therefore, the $t \times H$ and $a \times A$ models behave very differently in Fig. 1, describing a finite U, but not for $U = 0$, discussed below.

We observe that for a Hubbard U, the Coulomb interaction is independent of whether the electrons are in states with the same or different m-quantum numbers. Local pairing therefore does not cost Coulomb energy in this model. In a model which includes the Hund's rule coupling the situation is different, since the Hund's rule coupling acts against the Jahn-Teller effect. For the fullerides, however, the Jahn-Teller effect is stronger than the Hund's rule coupling [23] and therefore neglected here. Similar conclusions have been obtained by Capone *et al.* [24] using a somewhat different approach and different arguments.

We have so far focused on the effective interaction Γ. From Eq. (3) it is, however, clear that χ^0 is equally important. This quantity describes how pairs are propagated from site to site and how a coherent state is obtained. As the interaction is increased, spectral weight is transferred from the chemical potential, which tends to reduce χ^0. For the parameter range studied here, we therefore find that U tends to suppress superconductivity. Because of local pairing and the effects on Γ, however, this suppression is not nearly as efficient as might have been expected, as illustrated in Fig. 1.

2.5 $U = 0$. Migdal-Eliashberg theory

We now consider the case $U = 0$. Figure 3 shows T_c as a function of λ according to DMFT and Eliashberg theories. Since the phonon frequency is renormalized by the electron-phonon interaction, the Eliashberg calculation used a self-consistent phonon Green's function obtained from the lowest order phonon self-energy. Eliashberg theory is usually expected to overestimate T_c of doped C_{60} because of the violation [21] of Migdal's theorem. We find, however, that Eliashberg theory is quite accurate for both the $a \times A$ and $t \times H$ models for $U = 0$ and λ not too large. As λ is increased, spectral weight is transferred away from the chemical potential and χ^0 is reduced. This is also described by Eliashberg theory. For larger values of λ, however, the systems approach metal-insulator transitions. The reduction of χ^0 is then faster than predicted by Eliashberg theory, which then overestimates T_c. This happens for $\lambda \sim 0.6$ in the $a \times A$ model and for a larger λ in the $t \times H$ model. Although $\omega_{ph}/W = 0.25$ is not very small, and Migdal's theorem therefore is questionable, Migdal-Eliashberg theory agrees quite well with the DMFT results as long as the system is not close to a metal-insulator transition. It is also interesting that there is a small difference between the $t \times H$ and $a \times A$ models for $U = 0$.

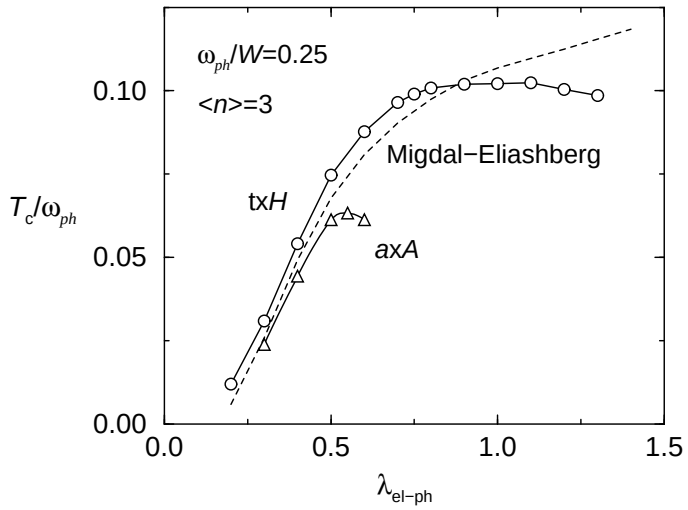

Fig. 3 T_c as a function of λ according to Migdal-Eliashberg (dashed line) and DMFT theories for the $t \times H$ ($\circ$) and $a \times A$ ($\triangle$) couplings at half-filling. The parameters are $\omega_{ph}/W = 0.25$ and $U = 0$ (after Han *et al.* [3]).

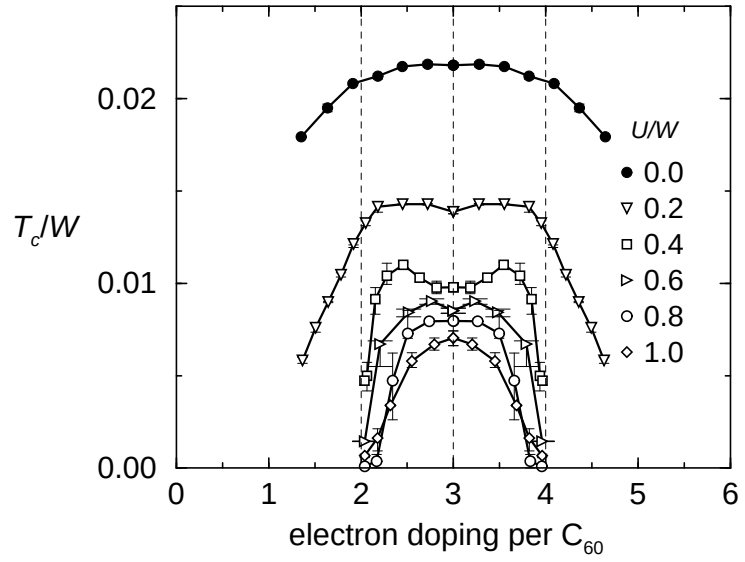

Fig. 4 T_c as a function of doping n for different values of U for $t \times H$ coupling. The parameters are $\omega_{ph}/W = 0.25$ and $\lambda = 0.6$. The figure illustrates the strong doping dependence for $U/W \geq 0.4$ (after Han *et al.* [3]).

2.6 Doping dependence

It is found experimentally that T_c drops quickly when the doping n deviates from $n = 3$ electrons per C_{60} molecule [25]. This cannot be explained within Eliashberg theory, since reducing the doping leads to a reduction of the Fermi energy and an increase in the density of states at the Fermi energy [26]. One would then actually expect an increase in λ and T_c according to Eliashberg theory.

Fig. 4 shows the doping dependence of T_c in the DMFT [3]. For small U, T_c drops slowly when the doping is reduced until $n \sim 2$ and then starts to drop much faster. Simultaneously, $\Gamma^{\rm loc}$ drops rapidly for $n < 2$, probably because the local pairing is inefficient once $n < 2$. For $U/W > 0.4$, T_c drops very quickly as $n = 2$ is approached from above. The reason is that the tendency for the system to become an insulator is much stronger for $n = 2$ than for $n = 3$ [27]. Whether or not the system actually becomes an insulator for $n = 2$, spectral weight is transferred away from the chemical potential. This leads to a reduction of χ_0, which causes a reduction of T_c. Despite strong local singlet formation near $n = 2$ and 4, the weak coherence from the reduced value of χ_0 lowers T_c.

3 Cuprates

3.1 t-J model

To describe phonons in cuprates, a t-J model with phonons [13, 14, 15, 16] can be derived from the three-band model [17]. The atoms in the three-band model are displaced, and the changes of the parameters in the t-J model are calculated to linear order in the displacements. By describing these displacements in terms of phonons, a t-J model with electron-phonon interaction is obtained. In the t-J model there is one site per Cu atom. These sites are occupied either by a $3d$-hole or a Zhang-Rice singlet, consisting of a $3d$-hole and an O $2p$-hole forming a singlet. The Hamiltonian is

$$\begin{aligned} H_{t\text{-}J} &= J \sum_{<i,j>} \left(\boldsymbol{S}_i \cdot \boldsymbol{S}_j - \frac{n_i n_j}{4} \right) - t \sum_{<i,j>\sigma} \tilde{c}^\dagger_{i\sigma} \tilde{c}_{j\sigma} + \sum_{\boldsymbol{q}\nu} \omega_\nu(\boldsymbol{q}) \left(b^\dagger_{\boldsymbol{q}\nu} b_{\boldsymbol{q}\nu} + \frac{1}{2} \right) \\ &\quad + \sum_{ij\sigma} \tilde{c}^\dagger_{i\sigma} \tilde{c}_{j\sigma} \sum_{\boldsymbol{q}\nu} g_{ij}(\boldsymbol{q},\nu)(b_{\boldsymbol{q}\nu} + b^\dagger_{-\boldsymbol{q}\nu}). \end{aligned} \tag{16}$$

Here $\tilde{c}^\dagger_{i\sigma}$ describes the creation of a $3d$-hole on site i and empty sites correspond to Zhang-Rice singlets. The operator $b^\dagger_{\boldsymbol{q}\nu}$ creates a phonon with wave vector $\boldsymbol{q}$, index ν and frequency $\omega_\nu(\boldsymbol{q})$. The formulas for $g_{ij}(\boldsymbol{q},\nu)$ have been given elsewhere [16]. Quadratic coupling terms have been neglected, although they can give some contribution to the doping dependence of the phonon energies.

This model can be solved for small clusters by using exact diagonalization. For small clusters, we can consider a Hilbert space which includes all electronic states. In addition we include all states where a maximum of K phonons have been excited, where $K \sim 5$. Within this space we find the ground-state $|0\rangle$ by using the Lanczos method. For this state the phonon spectral function $B_\nu(\boldsymbol{q},\omega)$ is calculated ($\omega > 0$)

$$B_\nu(\boldsymbol{q},\omega) = -\frac{1}{\pi} \mathrm{Im} \langle 0 | \phi_{\boldsymbol{q}\nu} \frac{1}{\omega - (H - E_0) + i0^+} \phi^\dagger_{\boldsymbol{q}\nu} | 0 \rangle, \tag{17}$$

where E_0 is the ground-state energy and $\phi_{\boldsymbol{q}\nu} = b_{\boldsymbol{q}\nu} + b^\dagger_{-\boldsymbol{q}\nu}$. Since the clusters are very small, the spectral function has only a few δ-functions. We therefore use the center of gravity to define the phonon energy. Since the results are rather sensitive to the boundary conditions, we consider periodic, anti-periodic and mixed boundary conditions, using periodic boundary conditions in one direction and antiperiodic boundary conditions in the other direction. We use the average result as the phonon frequency and the spread between the results as a measure of the accuracy.

The model (16) only describes the softening of phonons due to holes in the doped system, and it does not include other interactions present in both the doped and undoped systems. These interactions are described by a two-spring model, fitted to the phonon frequencies in the (1,0)- and (1,1)-directions of the *undoped* system. These experimental frequencies give $\omega_\nu(\boldsymbol{q})$ in Eq. (16), and the model therefore by construction gives correct frequencies for the undoped system.

Fig. 5 compares theory and experiment for a 4×4 cluster. It shows that the model correctly gives a strong softening for the half-breathing phonon in the $(1,0)$-direction and a weaker softening for the

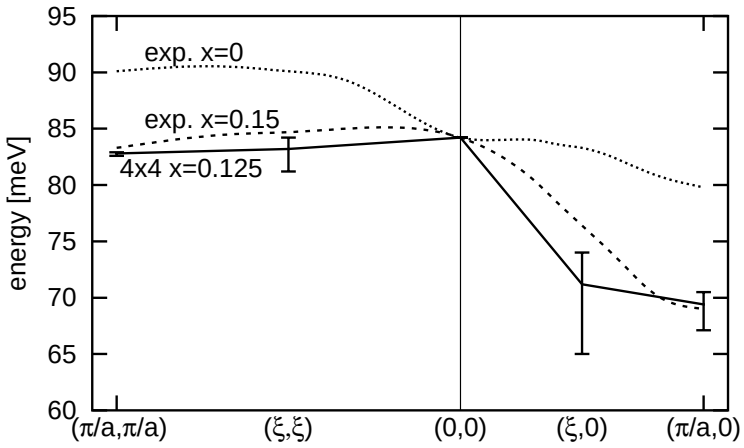

Fig. 5 Experimental (dotted line) and theoretical (full line) phonon dispersion in the (1,0) and (1,1) directions. Experimental results are given for $x = 0$ and $x = 0.15$ and theoretical results for $x = 0.125$. By construction, the model gives correct results for $x = 0$. The average over boundary conditions is shown and the bars show the spread due to different boundary conditions. The figure shows that there is a strong softening in the (1,0) direction, while the softening in the (1,1) direction is weaker. (after Rösch and Gunnarsson [16]).

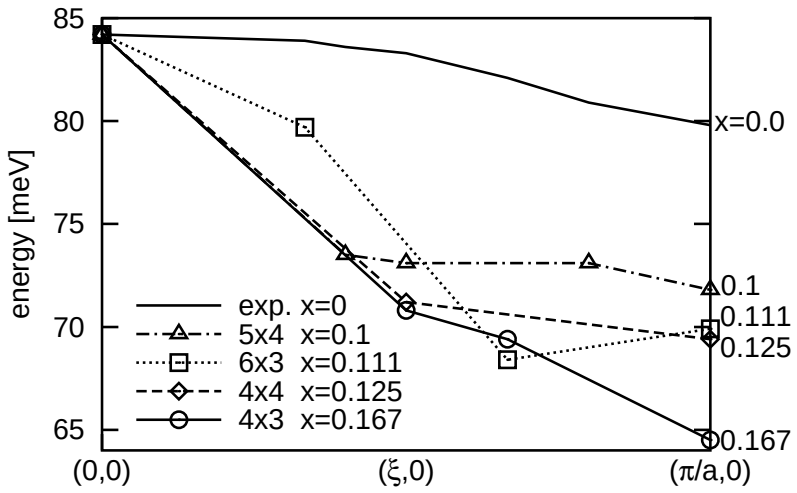

Fig. 6 Phonon dispersion in the (1,0) direction for different dopings. The figure illustrates that the softening increases with doping. (after Rösch and Gunnarsson [16]).

breathing phonon in the $(1,1)$-direction. The weaker softening in the $(1,1)$-direction follows since the phonon couples to electronic excitations with larger energies than for the $(1,0)$-direction. Fig. 6 shows the phonon softening in the (1,0)-direction for different cluster sizes. Since all clusters have two holes, the doping changes with cluster size. The fi gure shows that the softening increases with doping, in agreement with experiment [6].

3.2 Three-band model

As discussed in the introduction, LDA band structure calculations give accurate results for the energy of the half-breathing mode in the doped system [10], although the electron-phonon interaction $\lambda \sim 0.01$ is found to be very small [11, 10]. To study this further, we solve a three-band model of a CuO_2 plane in a mean-field HF approximation. Due to the mean-field character of the solution, one might expect it to show similarities to the LDA result. The HF approximation has the advantage, however, that the undoped system has an antiferromagnetic insulating solution. We can therefore also study the undoped system, and the softening under doping.

We use a three-band model with N unit cells

$$\begin{aligned} H &= \varepsilon_d \sum_{i\sigma} n_{id\sigma} + \varepsilon_p \sum_{j\sigma} n_{jp\sigma} + U \sum_i n_{id\uparrow} n_{id\downarrow} + \sum_{\langle i,j\rangle\sigma} [t_{ij}^{pd} \psi_{id\sigma}^\dagger \psi_{jp\sigma} + h.c.] \\ &\quad + \sum_{\langle i,j\rangle\sigma} t_{ij}^{pp} \psi_{ip\sigma}^\dagger \psi_{jp\sigma}, \end{aligned} \tag{18}$$

where $n_{id\sigma}$ and $n_{jp\sigma}$ are the occupation numbers for the N $3d$-orbitals and the $2N$ $2p-$orbitals, respectively, and $\psi_{id\sigma}$ and $\psi_{jp\sigma}$ are the corresponding annihilation operators. The site energies are ε_d and ε_p. The Coulomb repulsion between two $3d$-electrons on the same site is U. The model includes hopping between nearest neighbor Cu and O atoms and between the O atoms which are nearest neighbors of a particular Cu atom [28]. These hopping integrals have the absolute values t_{pd} and t_{pp}, respectively, with the signs determined by the relative orientations of the orbitals involved. The displacements of atoms change both electrostatic potentials and hopping integrals. The electrostatic potentials are screened differently in the doped and undoped systems. Since it was found that this does not strongly influence the half-breathing phonon [7], we only consider the change of hopping integrals.

The HF approximation involves the replacement

$$U \sum_i n_{id\uparrow} n_{d\downarrow} \to U \sum_{i\sigma} n_{id\sigma} \langle n_{id-\sigma}\rangle - U \sum_i \langle n_{id\uparrow}\rangle \langle n_{id\downarrow}\rangle. \tag{19}$$

leading to an effective level energy

$$\varepsilon_{id\sigma}^{\text{eff}} = \varepsilon_d + U \langle n_{id-\sigma}\rangle. \tag{20}$$

We use the parameters $t_{pd} = 1.6$ eV, $t_{pp} = 0$ and $U = 8$ eV. The level ε_p was adjusted so that the separation between the effective $3d$-level and $2p$-levels is about 3 eV.

Two calculations are performed, one for the undistorted lattice and one for a lattice where a phonon has been built in. This gives the second derivative, $\partial^2 E/\partial u^2$ of the total energy E with respect to a generalized phonon coordinate u. We can then obtain the softening of the phonon due to the interaction with the electrons in the model, reducing the frequency ω_{ph0} to ω_{ph}. The calculations were performed for a cluster of 32×32 CuO_2 units and periodic boundary conditions. We perform a calculation for the undoped system, having five electrons per unit cell, and allowing for spin-polarization. We adjust ω_{ph0} so that the softened frequency ω_{ph} is 0.080 eV for the zone boundary half-breathing phonon, as is found experimentally. The spin-polarized system has a large gap of about 4.6 eV. Due to this gap, the response of the system to a phonon is rather weak. The doped system is (assumed to be) paramagnetic, as found experimentally, and the response of the system is then larger. The result is a softening of the phonon.

Fig. 7 shows the doping dependence of the softening, which is found to be relatively weak [18]. For $\delta \sim 0.1$, the softening is of the right order of magnitude, but the doping dependence is substantially weaker than found experimentally or in the t-J model.

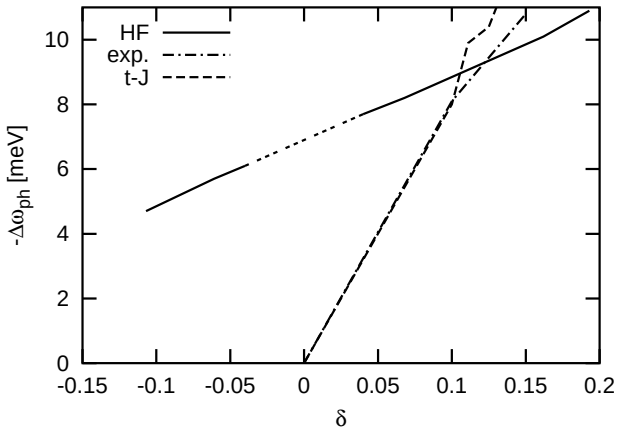

Fig. 7 Softening for the zone boundary half-breathing phonon in the HF approximation (full line), in the t-J model (dashed line) and according to experiment (dashed-dotted line) as a function of the hole doping δ. The few points in the t-J and experimental results have been connected by a line as a guide for the eye. The results for the HF approximation refer to the shift in a paramagnetic calculation for doping δ compared with an antiferromagnetic calculation for $\delta = 0$. The dashed part of the HF line indicates schematically that the systems goes antiferromagnetic for small dopings (after Rösch and Gunnarsson [18]).

The second derivative of the energy E can be expressed as

$$\frac{\partial^2 E}{\partial u^2} = \mathrm{Tr}\left(\frac{\partial H}{\partial u}\frac{\partial \rho}{\partial u}\right) + \mathrm{Tr}\left(\frac{\partial^2 H}{\partial u^2}\rho\right) \equiv \frac{\partial^2 E}{\partial u^2}^{(1)} + \frac{\partial^2 E}{\partial u^2}^{(2)}, \tag{21}$$

where H is the Hamiltonian and ρ is the density matrix.

We now focus on the contribution from $(\partial^2 E/\partial u^2)^{(1)}$, which can be compared [18] with the results in the t-J model. To make such a comparison, we project out the O $2p$ bands to obtain a one-band model, using a projection operator $P \equiv 1 - Q$. We apply the formula

$$\begin{aligned} &P(z-H)^{-1}P \\ &= [P(z-H)P - PHQ(z-QHQ)^{-1}QPH]^{-1}, \end{aligned} \tag{22}$$

where z is some typical energy. The modulation of the hopping integrals in the three-band model leads to a modulation of the level energies $\varepsilon_{id}^{\mathrm{One}}$ in the one-band model. In linear response one then has

$$\mathrm{Tr}\left(n_{id}\frac{\partial \rho}{\partial u}\right) = \frac{\partial \langle n_{id}\rangle}{\partial u} = \sum_j \chi_{ij}\frac{\partial \varepsilon_{jd}^{\mathrm{One,eff}}}{\partial u}, \tag{23}$$

where χ_{ij} is the response function for noninteracting electrons. $\varepsilon_{id}^{\mathrm{One,eff}}$ are the effective level energies of the one-band model in the HF approximation.

For the half-breathing mode at the zone boundary, the modulation of the level energies in the one-band model is

$$\pm 4 t_{pd}\frac{\partial t_{pd}}{\partial r}\frac{1}{\varepsilon_d^{\mathrm{One}} - \varepsilon_p}u, \tag{24}$$

where u is the phonon amplitude. The corresponding result in the t-J model is [16]

$$\pm 4 t_{pd}\frac{\partial t_{pd}}{\partial r}\left(\frac{2\lambda^2 - 1}{|\varepsilon_d - \varepsilon_p|} + \frac{2\lambda^2}{U - |\varepsilon_d - \varepsilon_p|}\right)u, \tag{25}$$

Table 1 Contributions to the phonon softening in the t-J model and in the HF solution of the three-band model. In the table we have for simplicity put $\varepsilon_d = 0$ (after Rösch and Gunnarsson [18]).

Source	t-J	HF	Ratio
Coupling	$[(2\lambda^2-1)/\lvert\varepsilon_p\rvert + 2\lambda^2/(U-\lvert\varepsilon_p\rvert)]^2$	$(1/\varepsilon_p)^2$	≈ 3
Sum rule	$\approx 2\delta\pi N$	$\approx \pi N$	$\approx 2\delta$
Denominator			≈ 1
Screening	1	≈ 0.5	≈ 2
Product			12δ

where $\lambda = 0.96$. The first term comes from the hopping of a $3d$-hole into the O $2p$-states and the second term from the hopping of a O $2p$-hole into the Cu $3d$-state. The second term has no correspondence in Eq. (24). Equation (25) has an additional factor 2 coming from a phase coherence factor in the Zhang-Rice singlet. This results from the singlet being explicitly written as a sum of two terms. Both these effects are genuine many-body effects. The -1 in the first term in Eq. (25) results from taking difference in the energy gain of a Zhang-Rice singlet and a single $3d$-hole.

The response function χ can be expressed in terms of a Kramers-Kronig relation

$$\mathrm{Re}\chi(\boldsymbol{q},\omega) = \frac{1}{\pi}\mathcal{P}\int d\omega' \mathrm{Im}\chi(\boldsymbol{q},\omega')\frac{1}{\omega-\omega'}, \tag{26}$$

where $\mathcal{P}$ means the principal value. There is a sum-rule for Im χ

$$\frac{1}{N}\sum_{\boldsymbol{q}\neq 0}\int_{-\infty}^{\infty}\left|\mathrm{Im}\chi(\boldsymbol{q},\omega+i0^+)\right| = \pi N\begin{cases}4n(1-n)\approx 1, & \text{noninteracting electrons;}\\ 2\delta(1-\delta), & t\text{-}J\text{ model.}\end{cases} \tag{27}$$

The approximate result for noninteracting electrons refer to the case when the filling of the band is $n = 0.5$, and the result for the t-J model is due to Khaliullin and Horsch [14]. The small value for the t-J model is due to a the hopping constraint in the t-J model and it is a many-body effect. The system can respond to a perturbation of a phonon by transferring charge carriers, i.e., Zhang-Rice singlets. Since there is only a fraction δ singlets and since they can only be transferred to sites without a singlet (fraction $1-\delta$), there is a factor $\delta(1-\delta)$. This strongly reduces the response in the t-J model.

We can now discuss the softening of the half-breathing phonon based on Eq. (26). In the t-J model, the on-site coupling $g_{ii}(\mathbf{q}) \equiv g(\mathbf{q})$ in Eq. (16) dominates for this mode. We therefore neglect the inter-site coupling. Then the phonon self-energy is given by

$$\Pi(\boldsymbol{q},\omega) = \frac{g(\boldsymbol{q})^2\chi(\boldsymbol{q},\omega)}{1+g(\boldsymbol{q})^2\chi(\boldsymbol{q},\omega)D_0(\boldsymbol{q},\omega)}, \tag{28}$$

where $D_0(\boldsymbol{q},\omega)$ is the noninteracting phonon Green's function. We find that the second term in the denominator is small for the parameters considered here. In the formal discussions below we therefore neglect it. The phonon self-energy is then proportional to the response function. For the effective one-band model, derived from the HF approximation for the three-band model, we obtain (Eqs. (21, 23))

$$\frac{\partial^2 E}{\partial u^2}^{(1)} = \sum_{ij}\frac{\partial\varepsilon_{id}^{\mathrm{One}}}{\partial u}\chi_{ij}\frac{\partial\varepsilon_{jd}^{\mathrm{One,eff}}}{\partial u}. \tag{29}$$

In both cases, the softening is given by a response function multiplied by coupling constants, given by Eq. (24) and Eq. (25). The coupling constants favor the softening in the t-J model by about a factor of three, as indicated in Table 1. At the same time, however, the response is suppressed in the t-J model

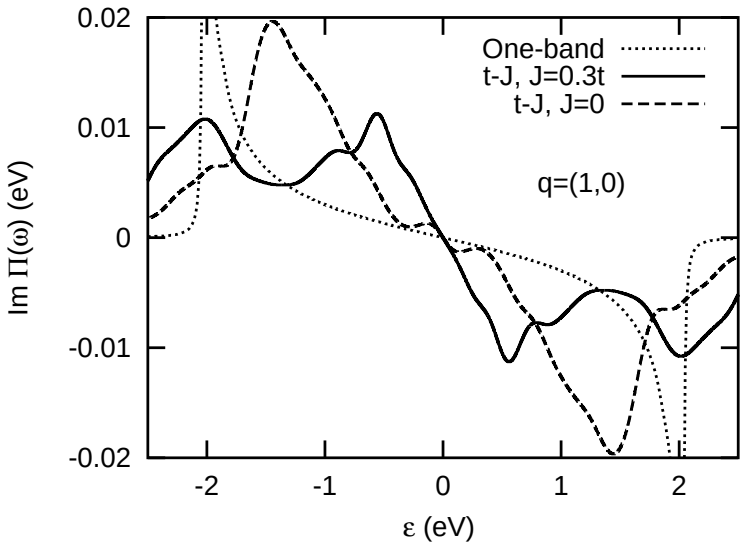

Fig. 8 Im $\Pi(\boldsymbol{q},\omega)$ for the $\boldsymbol{q}=(1,0)\pi/a$ half-breathing mode in the t-J model for $J/t=0.3$ (full line) and $J/t=0$ (dashed line) and in the one-band model (dotted line). The results for the t-J model were obtained for a 4×4 cluster. The self-energy has been given a Lorentzian broadening of 0.4 eV (full-width at half-maximum). The doping is $\delta=0.1$ (after Rösch and Gunnarsson [18]).

by the sum-rule (27), giving a factor 2δ (for δ small). The sum-rule refers to the imaginary part of the response function. The real part is obtained via a Kramers-Kronig transformation, and therefore the energy denominators play a role. We find that these denominators are comparable, favoring neither model. The coupling constant in Eq. (24) refers to the modulation of the on-site energies in the one-band model due to the modulation of the hopping integrals in the three-band model. One of the factors in Eq. (29), however, refers to the effective Hamiltonian, involving screening of the perturbation. This screening takes place because of charge transfers between the $3d$-levels and the resulting shift of the effective $3d$ levels in the HF approximation due to the Coulomb interaction. This reduces the HF response by about a factor of two. The result is that for $\delta\sim 0.1$, we expect the t-J and HF results for $(\partial^2 E/\partial u^2)^{(1)}$ to be comparable, as we also find in the calculations. The physics behind these results, however, is rather different.

To compare these approaches further, we have also considered the breathing mode, where all four O atoms surrounding a Cu atom move towards the Cu atom. For $\boldsymbol{q}=\pi/a(1,1)$ we find that the t-J model gives a weaker softening than for the half-breathing mode, in agreement with experiment. In the HF approximation, the model with $t_{pp}=0$ would give perfect nesting at half-filling and an unphysically large response to the breathing phonon. We have therefore introduced a finite $t_{pp}=1.1$ eV [28]. Even in this case, however, we find that the softening of the breathing phonon is stronger in the HF approximation than for the half-breathing phonon. A rather strong coupling to this mode was also found in an LDA band structure calculation [29].

To study the phonon width, we consider the imaginary part of the phonon self-energy Π. We first consider a simple model [18]. Since Im $\chi(\omega)\sim\omega$ for small ω, we assume

$$\mathrm{Im}\Pi(\boldsymbol{q},\omega)=\begin{cases}A\omega, & \text{if } |\omega|<W;\\ 0, & \text{otherwise,}\end{cases} \tag{30}$$

where A is some constant. From the Kramers-Kronig relation, it then follows

$$\frac{\gamma}{-\Delta\omega_{ph}} = \pi\frac{\omega_{ph}}{W}, \tag{31}$$

where $\gamma = 2\mathrm{Im}\Pi(\boldsymbol{q},\omega)$ is the full width at half maximum of the phonon and $\Delta\omega_{ph}$ is its shift. The HF approximation of the three-band model and the exact diagonalization solution of the t-J model give similar shifts $\Delta\omega_{ph}$. The band widths W are also similar in the two approaches. One may then also have expected that the phonon widths are similar.

To address this issue, we study the phonon self-energy [18]. From exact diagonalization, we obtain the phonon spectral function $B(\boldsymbol{q},\omega)$. The phonon Green's function $D(\boldsymbol{q},\omega)$ can then be obtained from a Hilbert transform. The phonon self-energy $\Pi(\boldsymbol{q},\omega)$ is obtained by inverting

$$D^{-1}(\boldsymbol{q},\omega) = D_0^{-1}(\boldsymbol{q},\omega) - \Pi(\boldsymbol{q},\omega), \tag{32}$$

where $D_0(\boldsymbol{q},\omega)$ is the noninteracting phonon Green's function. For a small system, the study of $\Pi(\boldsymbol{q},\omega)$ instead of $B(\boldsymbol{q},\omega)$ has important advantages. $B(\boldsymbol{q},\omega)$ has too few structure to allow the determination of peak widths. A broadened version of $\Pi(\boldsymbol{q},\omega)$, however, can give such information [18].

Figure 8 compares Im $\Pi(\boldsymbol{q},\omega)$ for the half-breathing phonon in the HF approximation of the one-band model and the exact solutions of a t-J cluster with $J/t = 0.3$ and $J/t = 0$. The figure illustrates how the introduction of the hopping constraints in the t-J model ($J/t = 0$) transfers spectral weight to smaller frequencies, by creating more low-energy excitations. This becomes even more pronounced for a finite J, since the interactions with the spins tends to create even more low-lying excitations. The result is a much larger broadening of the phonon in the t-J model than in the one-band model. Due to the small size of the clusters studied for the t-J model, the quantitative results are not reliable, but the trend of creating spectral weight at small frequencies is clear. We therefore find that although the HF approximation of the three-band model gives a softening of the right order of magnitude, both the doping and $\boldsymbol{q}$ dependences are incorrect and the broadening is too small.

4 Summary

This paper illustrates the importance of treating the Coulomb and electron-phonon interactions on an equal footing in strongly correlated systems. For alkali-doped fullerides, we find that the Migdal-Eliashberg theory breaks down. The main reason for this is not, however, that electron and phonon energy scales are comparable, as illustrated by Fig. 3. Instead, the break-down of the theory is mainly due to the closeness to a metal-insulator transition. This leads to a large transfer of spectral weight away from the chemical potential, which is not properly included in the Migdal-Eliashberg theory. The main finding is that in the presence of a large Coulomb interaction and for coupling to Jahn-Teller phonons, a local pairing of electrons on the C_{60} molecules becomes important. This makes superconductivity possible, although the phonon induced attraction is much weaker than the Coulomb repulsion. Such an interplay between Coulomb and electron-phonon interactions is not described by the Migdal-Eliashberg theory. The present theory naturally explains the strong doping dependence seen experimentally.

For cuprates, the large Coulomb interaction leads to a coherent hopping between the Cu $3d$- and O $2p$-levels. This results in a large Zhang-Rice singlet energy, which becomes important if the coupling to phonons is included [Eq. (25)]. This genuine many-body effect tends to enhance the electron-phonon coupling. At the same time the response of the system to a phonon is reduced [see Eq. (27)] by the hopping constraint but enhanced by the tendency of many-body effects to create low energy excitations (see Fig. 8). The result is a strong softening and broadening of the half-breathing phonon.

References

[1] G. Grimvall, *The Electron-Phonon Interaction in Metals* (North-Holland, Amsterdam, 1981).
[2] O. Gunnarsson, Rev. Mod. Phys. **69**, 575 (1997).
[3] J.E. Han, O. Gunnarsson, and V.H. Crespi, Phys. Rev. Lett. **90**, 167006 (2003).
[4] W. Metzner and D. Vollhardt, Phys. Rev. Lett. **62**, 324 (1989); M. Jarrell, Phys. Rev. Lett. **69**, 168 (1992); A. Georges, G. Kotliar, Krauth, and M.J. Rozenberg (1996) Rev Mod Phys **68**, 13 (1996).
[5] A. Lanzara, P. V. Bogdanov, X. J. Zhou, S. A. Kellar, D. L. Feng, E. D. Lu, T. Yoshida, H. Eisaki, A. Fujimori, K. Kishio, J.-I. Shimoyama, T. Noda, S. Uchida, Z. Hussain, Z.-X. Shen, Nature **412**, 510 (2001).
[6] S.L. Chaplot, W. Reichardt, L. Pintschovius, and N. Pyka, Phys. Rev. B **52**, 7230 (1995); L. Pintschovius, N. Pyka, W. Reichardt, A.Y. Rumiantsev, N.L. Mitrofanov, A.S. Ivanov, G. Collin, and P. Bourges, Physica C **185-189**, 156 (1991).
[7] L. Pintschovius and M. Braden, Phys. Rev. B **60**, R15039 (1999).
[8] L. Pintschovius and W. Reichardt, in *Neutron Scattering in Layered Copper-Oxide Superconductors*, edited by A. Furrer, Physics and Chemistry of Materials with Low Dimensional Structures, Vol. 20 (Kluwer Academic, Dordecht, 1998), p. 165.
[9] R.J. McQueeney, Y. Petrov, T. Egami, M. Yethiraj, G. Shirane, and Y. Endoh, Phys. Rev. Lett. **82**, 628 (1999).
[10] K.-P. Bohnen *et al.*, Europhys. Lett. **64**, 104 (2003) and priv. commun.
[11] S.Y. Savrasov and O.K. Andersen, Phys. Rev. Lett. **77**, 4430 (1996); O.K. Andersen, S.Y. Savrasov, O. Jepsen, and A.I. Liechtenstein, J. Low Temp. Physics **105**, 285 (1996).
[12] F.C. Zhang and T.M. Rice, Phys. Rev. B **37**, 3759 (1988).
[13] K.J. von Szczepanski and K.W. Becker, Z. Phys. B **89**, 327 (1992).
[14] G. Khaliullin and P. Horsch, Phys. Rev. B **54**, R9600 (1996); Physica C **282-287**, 1751 (1997); P. Horsch, G. Khaliullin and V. Oudovenko, Physica C **341**, 117 (2000).
[15] S. Ishihara and N. Nagaosa, cond-mat/0311200; Z.-X. Shen, A. Lanzara, S. Ishihara, and N. Nagaosa, Phil. Mag. B **82**, 1349 (2002).
[16] O. Rösch and O. Gunnarsson, Phys. Rev. Lett. **92**, 146403 (2004).
[17] V.J. Emery, Phys. Rev. Lett. **58**, 2794 (1987).
[18] O. Rösch and O. Gunnarsson, (to be publ.)
[19] A. N. Tahvildar-Zadeh, M. H. Hettler, and M. Jarrell, Phil. Mag. B **78**, 365 (1998).
[20] R. M. Fye and J. E. Hirsch, Phys. Rev. B **38** 433 (1988).
[21] J.K. Freericks, Phys. Rev. B **50**, 403 (1994).
[22] O. Gunnarsson, Phys. Rev. B **51**, 3493 (1995).
[23] G. Zimmer, M. Helmle, M. Mehring, and F. Rachdi, Europhys. Lett. **27**, 543 (1994); I. Lukyanchuk, N. Kirova, F. Rachdi, C. Goze, P. Molinie, and M. Mehring, Phys. Rev. B **51**, 3978 (1995); G. Zimmer, M. Mehring, C. Goze, and F. Rachdi, Phys. Rev. B **52**, 13300 (1995).
[24] M. Capone, M. Fabrizio, C. Castellani and E. Tosatti, Science **296**, 2364 (2002).
[25] T. Yildirim, L. Barbedette, J.E. Fischer, C.L. Lin, J. Robert, P. Petit, and T.T. M. Palstra, Phys. Rev. Lett. **77**, 167 (1996).
[26] M.P. Gelfand and J.P. Lu, Phys. Rev. Lett. **68**, 1050 (1992); Phys. Rev. B **46**, 4367 (1992); Phys. Rev. B **47**, 4149 (1993).
[27] J.E. Han, E. Koch, and O. Gunnarsson, Phys. Rev. Lett. **84**, 1276 (2000).
[28] O.K. Andersen, A.I. Liechtenstein, O. Jepsen, and F. Paulsen, J. Phys. Chem. Solids **56**, 1573 (1995).
[29] H. Krakauer, W.E. Pickett, and R.E. Cohen, Phys. Rev. B **47**, 1002 (1993).